# 9 Luminescence of disordered semiconductors



Disordered (amorphous) semiconductors are characterized by the absence of an ordered atomic arrangement over long distances from a chosen atom ('long-range order'). One is thus not allowed to employ the concepts familiar from the crystalline state such as the electron or hole wavevector $\mathbf{k}$, the Bloch theorem or the energy band structure perceived as the energy dependence of the charge carrier on the wavevector $\mathbf{k}$, i.e. $E = E(\mathbf{k})$. However, because the short range order (i.e. basically the periodic arrangement in the close surroundings of the given site) is kept, also the concepts of the conduction and valence bands, the forbidden gap and the density of states are basically conserved. These again are of decisive importance for understanding the luminescence processes, but the microscopic luminescence features in disordered solids differ quite considerably from the mechanisms that operate in their crystalline counterparts and that were discussed in Chapters 5, 7 and 8.

## 9.1 Densities of states in bands

The commonly accepted scheme of the electron and hole energy distribution in disordered semiconductors is depicted in Fig. 9.1(a): The electrons with energy higher than the so-called mobility edge $E_{cm}$ are considered free and may take part in the charge transport; their movement is characterized by the so-called microscopic mobility $\mu_m$. The electrons having energy $E < E_{cm}$ are not free; they are spatially localized in traps whose microscopic origin consists in deflections of the bond lengths and angles from their fixed values in a regular crystalline lattice. Upon applying an electric field these carriers can participate in the charge transport only via the so-called hopping mechanism, when the electrons tunnel between nearby potential wells that act as charge traps, or by means of so-called multiple trapping. In that case the localized electrons are thermally excited above the mobility edge $E_{cm}$, migrate with the mobility $\mu_m$, fall down into a distant trap, are thermally re-excited, etc. A mirror-like picture may be applied to the holes with relevant mobility edge $E_{vm}$.

The difference $E_{cm}$–$E_{vm}$ roughly corresponds to the energy bandgap in crystalline semiconductors. The density of states of the electrons with energy $E > E_{cm}$ is described by a square-root function $\rho(E) \simeq (E - E_{cm})^{1/2}$, analogously to crystals. In an ideal crystalline semiconductor, however, the density of states within the bandgap is zero, while in disordered materials it remains non-zero even for $E < E_{cm}$. It has been established that the density of these states (originating, as already mentioned, owing to variations of the bonding parameters between atoms), $g(E)$, drops exponentially downwards from the mobility edge [1]



$$g_c(E) = g_{c0} \exp(-E/E_{c0}). \tag{9.1}$$

In this expression the energy $E$ is referred to $E_{cm}$ and considered positive downwards, see Fig. 9.1. A similar convention for the holes yields

$$g_v(E) = g_{v0} \exp(-E/E_{v0}). \tag{9.2}$$

The quantities $E_{c0}$, $E_{v0}$ stand for the energy widths of the tail states (i.e. the states extending into the 'energy gap') of the conduction and valence bands, respectively. They amount typically to tens of meV. Nonequilibrium electron–hole pairs, created with the generation rate $G$, rapidly thermalize (within $10^{-13}$–$10^{-12}$ s) towards the corresponding mobility edges, then deeper into the tail states and eventually—on a much longer timescale—they may recombine radiatively via tunnelling between nearby sites with a recombination rate $1/\tau_r$ (Fig. 9.1(b)). This is generally believed to be the main radiative recombination channel in disordered semiconductors.

Within the bandgap of disordered semiconductors one can find other electron states. The deformed covalent bonds between neighbouring atoms are exposed to mechanical strain and may break. This rupture gives rise to so-called dangling or unsaturated bonds. They are very often passivated by hydrogen atoms (especially in hydrogenated amorphous silicon, a-Si:H), but some remain unpassivated, may capture an electron and thereby introduce deep localized electron states approximately in the middle of the bandgap. Important, from the luminescence standpoint, is that these deep defect levels act as efficient centres of *non-radiative recombination* (Fig. 9.1(b)), which is, after all, a general property of all deep defect states (see Chapter 6).

It should be noted also that the total density of the dangling bonds is not constant in time. It grows upon irradiating the sample with photons $h\nu \geq E_{cm} - E_{vm}$ that create free electron–hole pairs. Subsequent non-radiative recombination of these *e–h* pairs may release energy sufficient to break the weakened bonds, as explained already in Section 6.2. The process has been known for a long time as the Staebler–Wronski effect [2] but its microscopic mechanism has not been understood in all details till now. Recent results indicate that it is basically due to bimolecular non-radiative recombination [3].

The dangling bonds can be either empty (i.e. positively charged, $D^+$, because the negative electron charge is missing there), or occupied with one electron ($D^0$), or with two electrons of opposite spins (negatively charged dangling bond, $D^-$). The energy required to add the second electron to an already occupied dangling bond is called the correlation energy $U$, see Fig. 9.1(a).

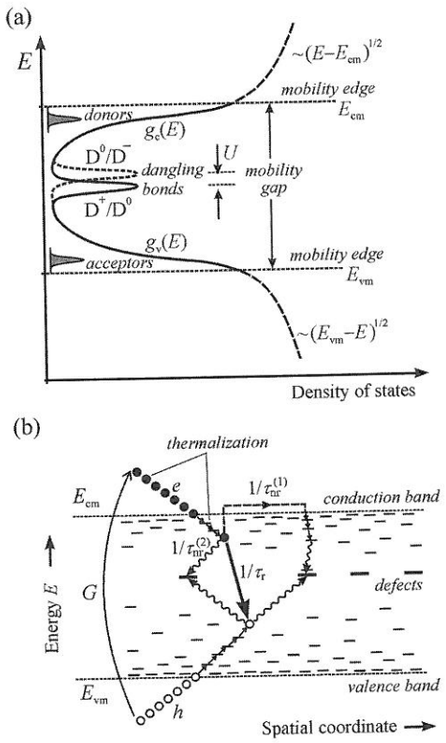


**Fig. 9.1**
(a) Schematic of the electron density of states in disordered semiconductors. Luminescence properties are mainly driven by occupation of the localized, so-called tail states $g_c(E)$, $g_v(E)$ that drop exponentially down from the relevant mobility edges into the 'forbidden' gap. The electrons above the mobility edge $E_{cm}$ occupy free states, whose density is described approximately by a square-root shape (like the holes below the $E_{vm}$ edge). Approximately in the middle of the bandgap there are levels $D^+$, $D^0$, $D^-$ arising from the dangling bonds. These levels represent efficient non-radiative centres. (b) Schematic of thermalization and recombination of non-equilibrium electrons and holes in amorphous semiconductors. The radiative recombination of an $e$–$h$ pair localized in the tail states ($1/\tau_r$) competes with non-radiative tunnelling to a deep defect level ($1/\tau_{nr}^{(2)}$) or with non-radiative recombination due to thermal carrier excitation and subsequent diffusion towards the non-radiative centres ($1/\tau_{nr}^{(1)}$).

The last types of energy levels in disordered semiconductors are possible impurity levels in doped materials. These are located, similarly to crystalline counterparts, within the bandgap close below the relevant mobility edges (donors and acceptors in Fig. 9.1(a)).

## 9.2 Temperature dependence of luminescence

We have seen that the disorder does not introduce any new kinds of recombination processes fundamentally different from crystalline solids. However, the radiative recombination in the tail states exhibits a typical experimental dependence whose provenance can be simply derived. We start with the expression for luminescence quantum efficiency (3-2) by rewriting it as a relation suitable for the luminescence intensity as a function of temperature $I(T)$:

$$I(T) = I_0 \frac{p_r(T)}{p_r(T) + p_{nr}(T)} = I_0 \frac{1/\tau_r}{(1/\tau_r + 1/\tau_{nr})}. \tag{9.3}$$

Here $p_r$ and $p_{nr}$ stand for the probability of radiative and non-radiative recombination, respectively, and $\tau_r$ and $\tau_{nr}$ denote the corresponding recombination times. $I_0$ is a constant quantity whose meaning will be discussed below.



Expression (9.3) simply connects the luminescence intensity with its quantum efficiency $\eta$, namely, $I(T) = I_0\eta(T)$.

At a fixed temperature, the electron (or hole) in the tail state with energy $E$ can, according to Fig. 9.1(b), either recombine radiatively ($1/\tau_r$) or be excited thermally above the mobility edge and subsequently diffuse towards a non-radiative centre ($1/\tau_{nr}^{(1)} \equiv 1/\tau_{nr}$).[1] Thermal excitation causing luminescence quenching is described by the known relation (4.17) that now reads

$$1/\tau_{nr} = p_0 \exp(-E/k_B T), \tag{9.4}$$

where $p_0 \approx 10^{12}\ s^{-1}$ is the so-called frequency factor. The electrons and holes in shallow states ($E$ small) thus recombine mainly non-radiatively, while the photocarriers deep below the relevant mobility edge have no chance to 'escape non-radiatively' and rather they give rise to recombination luminescence radiation. It is thus possible to define a temperature dependent *demarcation energy* $E_D(T)$; carriers at this energy have the rate of radiative recombination just equal to the rate of non-radiative recombination given by (9.4):

$$1/\tau_r = p_0 \exp(-E_D(T)/k_B T). \tag{9.5}$$

The significance of the demarcation energy therefore consists in separating light-emitting states from non-radiative ('dark') states.

Now we can express the quantum efficiency through the tail state densities as

$$\eta = \frac{p_r(T)}{p_r(T) + p_{nr}(T)} = \frac{\int_{E_D}^{\infty} g_v(E)\mathrm{d}E}{\int_0^{\infty} g_v(E)\mathrm{d}E} = \mathrm{e}^{-E_D(T)/E_{v0}}. \tag{9.6}$$

The integrals in (9.6) mean summing over all the tail states ($\int_0^{\infty} \mathrm{d}E$) and over the states below the demarcation energy ($\int_{E_D}^{\infty} \mathrm{d}E$). Note that we sum over the valence band states (9.2) only. This is justified by different widths of the tail states: The valence band tail states are usually wider than the conduction band ones ($E_{v0} > E_{c0}$). Consequently, even if both kinds of photocarriers located above the relevant demarcation energy may be thermally released, decisive for the efficiency of the non-radiative process is the release of deeper lying holes—the electrons liberated easily from their shallower states cannot recombine unless free holes, upon migrating through the sample, occupy the deep centres of non-radiative recombination.

Supposing further that $\eta$ is very small compared with unity (i.e. $p_{nr}(T) \gg p_r(T)$, or $\eta = p_r/(p_r + p_{nr}) \approx p_r/p_{nr}$), expression (9.3) becomes

$$\frac{I_0}{I(T)} = \frac{I_0}{I_0 p_r/(p_r + p_{nr})} = \frac{p_r + p_{nr}}{p_r} = 1 + \frac{p_{nr}}{p_r} \cong 1 + \frac{1}{\eta}$$

[1] For the sake of simplicity we neglect here the (temperature independent) channel of direct non-radiative recombination $1/\tau_{nr}^{(2)}$.

or

$$\left(\frac{I_0}{I(T)} - 1\right) \cong \frac{1}{\eta},$$

which, with the aid of (9.6), yields the required expression for the characteristic temperature dependence of luminescence

$$\ln\left(\frac{I_0}{I(T)} - 1\right) = \frac{E_D(T)}{E_{v0}} \equiv \frac{T}{T_0}. \tag{9.7}$$

In (9.7) we have introduced, to a certain extent formally, the characteristic temperature $T_0$ via

$$E_{v0} = k_B T_0 \ln(p_0 \tau_r). \tag{9.8}$$

Such a definition of $T_0$ can be justified by a formal similarity of $E_{v0}$ and $E_D(T)$, provided we express the latter quantity from eqn (9.5). The parameter $T_0$ characterizes the width of the tail states.

Therefore, plotting the experimentally acquired values of $\ln(I_0/I(T)–1)$ against $T$ should yield—provided the above model is correct—a straight line with slope $1/T_0$. The curves in Fig. 9.2(a), measured in various samples of hydrogenated amorphous silicon, nicely demonstrate that this is the case [4]. The reciprocal slope value $T_0$, extracted from this figure, amounts to $T_0 = 22$–$23$ K. The parameter $T_0$ is very sensitive to the degree of disorder: In amorphous alloys, where, besides the topological disorder, also composition disorder occurs (e.g. in a-Si:H with high hydrogen content $\geq$ 10 at. %) the tail states are much wider. Figure 9.2(b) shows the dependence (9.7) for a-Si:H with 19 at. % of hydrogen [5]. The slope of the linear plot yields $T_0 = 62$ K. This means that, among others, the photocarriers after thermalization get localized in deep states and thus the thermal luminescence quenching is less effective. This corroborates Fig. 9.2(b)—it becomes evident that $I(T) \neq 0$ even at room temperature while in 'standard' a-Si:H with hydrogen content of about 5–10 at.% only, photoluminescence at $T = 295$ K in fact does not occur. The presence of room-temperature luminescence in amorphous alloys is supported probably also by a low carrier mobility, which makes the 'search' of released carriers for non-radiative centres more difficult.

Till now, we have not specified how to assess the constant $I_0$ and what is its meaning. This can be easily anticipated—since monotonic thermal luminescence quenching is involved with increasing temperature, as indicated, e.g. by the growth of the demarcation energy with temperature (9.5), $I_0$ should mean the luminescence intensity at the lowest temperature of measurement. (After all, it can be deduced from (9.7) that $I_0/I(T) > 1$ must always hold, for formal reasons.) Despite this, the assessment of $I_0$ may be ambiguous in some cases, because in disordered semiconductors the form of $I(T)$ at the lowest temperatures (about 4–70 K) is not always simple: Sometimes in this temperature range a 'plateau' is found; another time even a moderate increase of $I(T)$ with increasing temperature is observed. The question then arises which value of $I(T)$ to select as $I_0$. This selection may influence the left part of the curve $[I_0/I(T)–1]$, as becomes evident in Fig. 9.2(b) for the



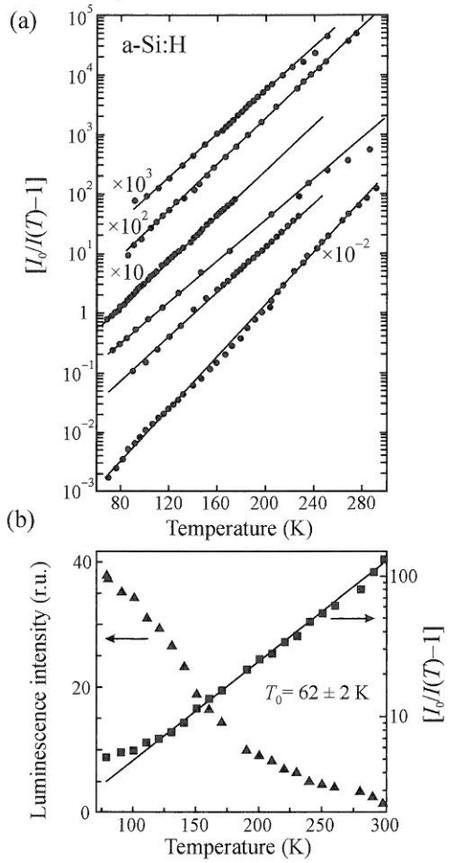


**Fig. 9.2**
(a) Plot of $[I_0/I(T)–1]$ against $T$ in samples of a-Si:H prepared in various ways. After Collins *et al.* [4]. (b) The same plot (■) obtained in an a-Si:H alloy with high hydrogen content. Also the direct dependence of $I(T)$ on temperature is shown (▲). After Luterová *et al.* [5]. The symbols denote experimental data, and the lines are fits according to (9.7).

data at $T \leq 125$ K. For a more detailed discussion, the reader is referred to the literature [4]. Of course, $I_0$ is only a certain experimental parameter, not (unlike the fit parameter $T_0$) a characteristic material constant.

The model under discussion leads to the following consequence: The demarcation energy $E_D(T)$ increases with increasing temperature. Therefore, the luminescence emission spectrum as a whole (or its maximum) must shift to the red and, what is of the essence, this shift must exceed the temperature redshift of the bandgap. Figure 9.3 shows that this is the case [6].

Let us now attempt to summarize all assumptions applied in deriving the temperature behaviour (9.7) and to determine the limits of its validity. First, as we have just stated, this model can be applied only in a temperature range where the luminescence intensity drops with increasing $T$. Besides, we have neglected the channel of direct non-radiative tunnelling ($1/\tau_{nr}^{(2)} = 0$). This, it is true, means implicitly that within the model the quantum efficiency $\eta$ is equal to unity, provided the photocarriers thermalize into states lying below the demarcation energy. This may occur at sufficiently low temperatures when no carriers can be thermally excited to the free states, and thus all they can do

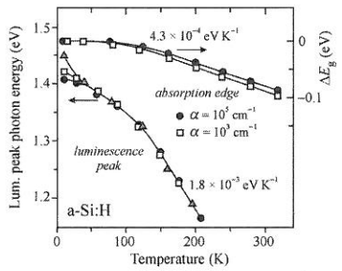


**Fig. 9.3**
Temperature shift of the emission band maximum in a-Si:H (with rate of $1.8 \times 10^{-3}$ eV/K; different symbols denote different samples or different excitation modes) in comparison with the temperature shift of the absorption edge ($4.3 \times 10^{-4}$ eV/K). After Tsang and Street [6].

is to recombine radiatively. This fact, however, gets involved in a contradiction with the second assumption applied in deriving (9.7), namely, that $\eta \ll 1$. Is the model thus inconsistent?

It is better to say one should be cautious in making use of it. The mentioned contradiction may be removed if we admit $1/\tau_{nr}^{(2)} \neq 0$. The overall character of $I(T)$ remains unchanged, but the left-hand side of the definition (9.5) of the demarcation energy will comprise the low-temperature luminescence decay rate $1/\tau_L^0 = 1/\tau_r + 1/\tau_{nr}^{(2)}$ instead of the reciprocal radiative lifetime $1/\tau_r$. Similarly, $\tau_L^0$ will substitute for $\tau_r$ in expression (9.8) for $E_{v0}$. We have to keep this in mind when deriving $E_{v0}$ from the experimentally determined $T_0$, and also in a possible reciprocal procedure: if, for instance, we assess $E_{v0}$ via optical absorption or photoelectric measurements (in addition to evaluating $T_0$ from luminescence experiments), we have to carefully analyse every time whether eqn (9.8) will yield $\tau_r$ or $\tau_L^0$. This difference is not always sufficiently accentuated in the literature.

## 9.3 Distribution of luminescence lifetimes

In the preceding section we implemented for disordered semiconductors a single luminescence decay time $\tau_L$, in full analogy with their crystalline counterparts. This is, however, an oversimplification that does not correspond to the facts. In disordered materials, generally speaking, a large range of luminescence decay times occurs, spanning from $10^{-9}$ s up to $10^{-1}$ s, in strong dependence upon temperature. The reason for this consists in the fact that the tail states, in which luminescence originates, are very broad and have a very variable spatial density.

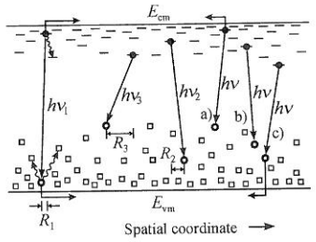


**Fig. 9.4**
Illustrating the distribution of luminescence decay times. The conduction band tail states are depicted by short horizontal lines, those of the valence band by squares (the tail state widths are exaggerated for the sake of clarity). Oblique arrows represent radiative recombination via tunnelling, horizontal arrows denote the escape of carriers towards non-radiative centres and the wavy lines indicate carrier thermalization.

The non-equlibrium electrons sitting in energy states close to the mobility edge $E_{cm}$ can find in their close neighbourhood many 'deep' hole states (in proximity to $E_{vm}$) for tunnelling radiatively. That is, near the mobility edges the densities of states (9.1) and (9.2) acquire their maximal values per unit volume. Because the probability of radiative tunnelling can be expressed as $1/\tau_r \approx \exp(-2R/R_0)$, where $R$ is the localized electron–localized hole separation and $R_0$ is a characteristic constant, this probability is large for small $R$. Therefore, high-energy luminescence photons $h\nu_1$, corresponding to a small distance $R_1$, will decay faster than photons $h\nu_2 < h\nu_1$ and $h\nu_3 < h\nu_2$ that belong to the tunnelling separations $R_2 > R_1$ and $R_3 > R_2$ (Fig. 9.4).

Furthermore, energetically higher lying carriers find more chance to thermalize (wavy lines) and also to escape non-radiatively into the free states (Fig. 9.4, left part). This, altogether, makes the high-photon-energy luminescence radiation decay faster that the low-energy radiation. Consequently, a continuous distribution of luminescence decay times $g(\tau_L)$ must exist; taking into account its considerable width, it is usually plotted as a function of the logarithm of the decay time $g(\log \tau_L)$.

The luminescence of every electron–hole pair localized in the tail states can certainly be regarded as a 'monomolecular' type of radiative recombination,



i.e. according to (3.5) we shall consider the individual decay curves in the form

$$i_L(t) = i(0)e^{-t/\tau_L} = \frac{N_0\eta}{\tau_L}e^{-t/\tau_L}, \tag{9.9}$$

where $N_0$ denotes the number of excited centres ($e$–$h$ pairs with the decay time $\tau_L$) and $\eta$ stands for the luminescence efficiency. However, owing to the existence of $g(\log \tau_L)$, instead of (9.9) we now have to consider the sum over all possible $\tau_L$:

$$i_L(t) = \eta N_0 \int_{-\infty}^{+\infty} d(\log \tau_L) g(\log \tau_L) \frac{\exp(-t/\tau_L)}{\tau_L}. \tag{9.10}$$

An example of an experimentally acquired distribution $g(\log \tau_L)$ is shown in Fig. 9.5 [7].

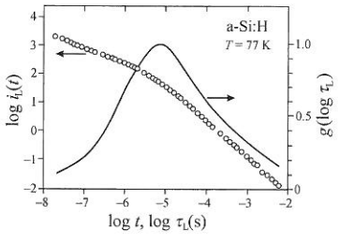


**Fig. 9.5**
Temporal shape of the decay of the spectrally integrated photoluminescence of a-Si:H at a temperature $T = 77$ K (symbols) and the relevant decay time distribution $g(\log \tau_L)$ (full curve) defined via (9.10). After Wang and Fritzsche [7].

Now we analyse how to determine the distribution function $g(\log \tau_L)$ experimentally. One of the possible ways is as follows. We have mentioned in Section 3.4 that the luminescence decay curve in disordered systems can be in most cases described phenomenologically by the temporal stretched exponential function

$$i_L(t) = i(0)\exp[-(t/\tau)^\delta], \tag{9.9a}$$

where $\tau$ is called the decay time and $\delta \in (0, 1\rangle$ is the so-called dispersion factor. Now, let us recall the definition of the Laplace transform of a function $f(x)$

$$F(t) = \int_0^\infty f(x)e^{-tx}dx;$$

$x$ is a real argument and $F(t)$ is called image of the Laplace transform. Substituting $x = 1/\tau$ yields

$$F(t) = \int_0^\infty f(1/\tau)\exp(-t/\tau)\frac{d\tau}{\tau^2}$$

and, if in (9.10) we write $d(\log \tau_L) \approx d\tau_L/\tau_L$ and replace formally $g(\log \tau_L) \to f(1/\tau_L)$, eqn (9.10) becomes

$$i_L(t) \approx \int_0^\infty f(1/\tau_L)\exp(-t/\tau_L)\frac{d\tau_L}{\tau_L^2}. \tag{9.10a}$$

By comparing (9.9a) with (9.10a) it turns out that, under suitable normalization, one can write

$$\exp\left[-(t/\tau)^\delta\right] = \int_0^\infty f(1/\tau_L)\exp(-t/\tau_L)\frac{d\tau_L}{\tau_L^2}. \tag{9.10b}$$

The last equation implies that, in order to reveal the distribution function $f(1/\tau_L)$, first of all we should determine $\tau$, $\delta$ by virtue of fitting the

experimental decay curve $i_L(t)$, and then we can calculate $f(1/\tau_L)$ as the inverse Laplace transform of the stretched exponential function.[2]

This procedure is applied whenever the distribution functions $g(\tau_L)$ or $f(1/\tau_L)$ are relatively narrow. An example will be given in Chapter 15 (Fig. 15.1). When the distribution function is sufficiently broad ($g(\log \tau_L)$), it can be determined by making use of a much simpler way, namely, directly from the measured decay curve $i_L(t)$ as $g(\log \tau_L) \simeq i_L(t)t$ (Problem 9/3).

The preceding discussion on the continuous character of $g(\log \tau_L)$ has not been fully exhausting. Even if we study the 'monochromatized' luminescence of disordered semiconductors, i.e. if we measure the decay time on a single selected wavelength, we obtain curves $g(\log \tau_L)$ similar to those displayed in Fig. 9.5, see Fig. 9.6(a) [8]. Referring to what has been said above this could hardly be expected (!) How, then, is it possible?

The answer is given in Fig. 9.4. The recombination of the *e–h* pairs (a) and (c) will be faster than that of the pair (b), because both the electron in case (a) and the hole in case (c) can be easily thermally excited into delocalized states and subsequently find a counterpart to recombine non-radiatively. At the same time the photon energy $h\nu$ may be in all three cases (a), (b) and (c) identical. Moreover, the random statistical distribution of the electron–hole separation $R$, occurring also for $h\nu = \text{const}$, will manifest itself.

In materials where the tail state widths $E_{v0}$ and $E_{c0}$ are large enough, the luminescence is present till room temperature. This is expected to be due to participation in the radiative recombination of predominantly those electrons and holes which are localized deepest in the bandgap. In this case we may expect a sizeable narrowing of $g(\log \tau_L)$. The inset in Fig. 9.6(b) [5] or its comparison with the curves shown in Fig. 9.6(a) demonstrate that this is indeed the case.

## 9.4 Spectral shape of the emission band

Figure 9.7 displays examples of photoluminescence emission spectra of several pure amorphous semiconductors [9–11]. All of these spectra exhibit a simple structureless band of considerable width (FWHM $\approx$ 200–400 meV). Its shape is approximately Gaussian—with a minor asymmetry towards low photon energies—and does not exhibit any indications of a potential fine structure.

To explain this spectral shape, firstly we shall attempt to apply some of the models discussed in previous chapters. However, because of the different microscopic essence and different density of the electronic states, participating in the radiative recombination in the amorphous and crystalline phases, it is not at all obvious whether we shall succeed. For instance, it stands to reason that the model of free *e–h* pairs (Section 5.2) is inapplicable, since now the light emission originates in *localized* states. Besides, the observed bandwidth is much larger than the corresponding Boltzmann factor $\sim k_B T$

[2] It is worth stressing that if the left-hand side of (9.10b) contains the stretched exponential function, the distribution $f(1/\tau_L)$ cannot be analytically expressed via simple functions such as the Gaussian distribution, etc.



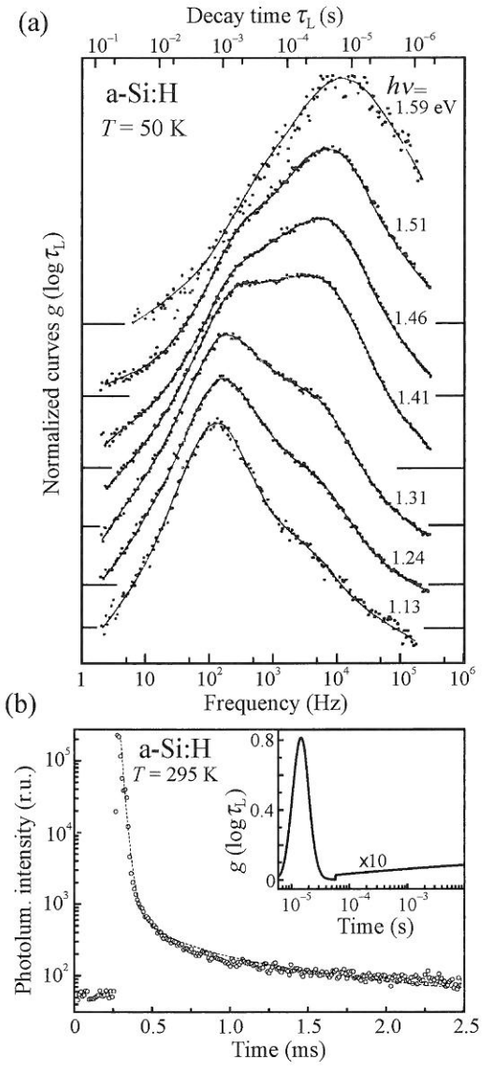


**Fig. 9.6**
(a) The distribution function $g(\log \tau_L)$ of photoluminescence of a-Si:H for various emitted photon energies at $T = 50$ K, after Oheda [8]. To acquire $\tau_L$, the method of phase shift (Subsection 2.9.2) was used; the lower abscissa represents the modulation frequency of the excitation radiation. (b) The photoluminescence decay curve in an amorphous alloy a-Si:H with 19 at.% of hydrogen, room temperature. The inset demonstrates narrow distribution function $g(\log \tau_L)$. After Luterová *et al.* [5].

($\approx$ 25 meV at room temperature). For a similar reason we have to reject the radiative recombination of type e–$A^0$ or h–$D^0$ (Section 5.3). Excitons as the quasi-particles with a well-defined wavevector do not exist in amorphous materials, thus we are not allowed to apply any of the channels of the exciton luminescence, discussed in Chapter 7. The broad emission band could perhaps correspond to electron–hole liquid EHL (Section 8.4) or electron–hole plasma EHP luminescence (Section 8.5), but these are high-excitation effects while in disordered semiconductors this kind of light emission occurs independently of the excitation intensity and, moreover, it exhibits its specific temperature behaviour (Section 9.2) that is incompatible with the EHL or EHP models.

And yet, there remains one possibility. A broad structureless emission band can occur at the localized optical centre with a strong electron–phonon coupling (Section 4.5). In disordered semiconductors, the non-equilibrium carriers actually become localized before recombination and, to employ the configuration coordination concept, there is no need to meet the presumption about the long-term ordering (i.e. a regular crystalline lattice). This is the basic idea underlying the *phonon broadening* model, which has been submitted to interpret the broad emission band in a-Si:H by Street [12]. This concept therefore assumes that each *e–h* pair localized in the tail states has a strong phonon interaction with the surrounding matrix, which leads to a large Huang–Rhys factor $S \gg 1$ (or to a Debye–Waller factor $u_{DW} = 0$), to the absence of the no-phonon line and the appearance of a broad Gaussian emission band with a considerable Stokes shift. The bandshape is then described by (Appendix F)

$$I_{sp}^{a}(h\nu) \approx \text{const} \exp\left\{-\frac{[h\nu - (E_0 - E_R)]^2}{2\sigma^2}\right\}, \qquad (9.11)$$

where $E_0$ is the transition no-phonon energy, $E_R = S\hbar\omega$ stands for the relaxation energy ($\hbar\omega$ being the phonon energy) and $\sigma$ denotes the band halfwidth at the points of inflection.

Indeed, the emission band maximum in a-Si:H peaks at $\sim 1.4$ eV (Fig. 9.7), while the optical bandgap width amounts to $\sim 1.9$ eV. The shift in the luminescence maximum from the absorption edge thus amounts to $2E_R \sim 0.5$ eV. Enumerating the FWHM of the band, which is described by eqn (9.11), through relation (F-4), yields $\sigma_F = 4\sqrt{\ln 2 E_R \hbar\omega} \approx 370$ meV if we consider $E_R = 250$ meV and adopt $\hbar\omega = 50$ meV as a typical phonon energy. Everything

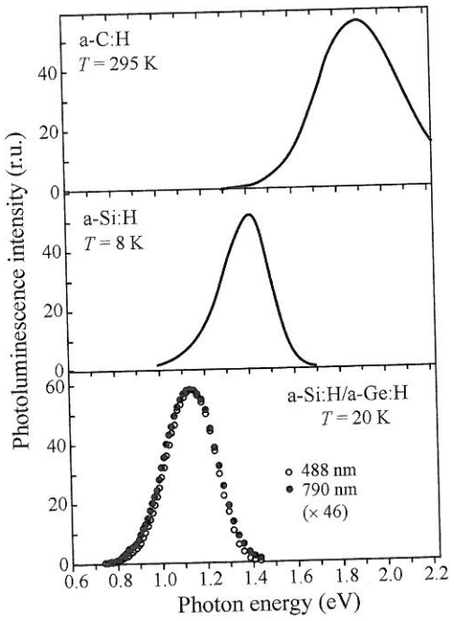


**Fig. 9.7**
Examples of the emission spectra of undoped hydrogenated amorphous semiconductors. From the top downwards: a-C:H (after Koós *et al.* [9]), a-Si:H (after Street and Biegelsen [10]) and multilayers a-Si:H (5 nm)/a-Ge:H (1 nm) (after Deki *et al.* [11]). The lowermost curve documents independency of the spectral shape of the excitation wavelength ($\lambda_{ex} = 488$ nm and $\lambda_{ex} = 790$ nm were applied). Notice also different measurement temperatures.



corresponds well to experimental data. The phonon broadening model thus reasonably describes the dominant spectral features, however, at the same time it involves implicitly the assumption about a fixed value of the no-phonon energy of all of the recombining *e–h* pairs (at most, the model can allow for a very narrow distribution of these energies only); otherwise an additional inhomogeneous broadening due to disorder would arise. This assumption is open to discussion and, in fact, denies to a large extent the effect of the finite width of the tail states. Moreover, the experimentally observed emission band is not fully symmetric but exhibits a slight low-energy tail.

Therefore, a diametrically opposite approach to the interpretation of the emission band—particularly in a-Si:H again—has been taken by Dunstan and Boulitrop [13, 14]. They have proposed a model of *disorder broadening* in which the tail states are supposed to be quite 'solid', i.e. without any electron–phonon interaction, and the sizeable emission bandwidth is interpreted as being due to a wide distribution of these states. Here, an idea might cross our mind, namely, that the authors copy the procedure we used previously to derive the spectral shape of the luminescence of free *e–h* pairs in indirect crystalline semiconductors (Subsection 5.2.2): the convolution of occupied electron and hole states, this time in the relevant tail states instead of in the conduction and valence bands.[3] It is thus tempting to adopt relation (5.10) in which we merely replace the square root functions by the exponential expressions (9.1) and (9.2).

However, we are not allowed to proceed in this way. Amorphous semiconductors, as already stressed several times, have their specific features. Above all, the tunnelling radiative lifetime $\tau_r$ is not constant but depends strongly on the electron–hole separation. The transition matrix element thus cannot be put outside the integral. In addition, in amorphous materials it is possible, no doubt, to introduce the Fermi–Dirac distribution function for electrons and holes, but not all the non-equilibrium *e–h* pairs are able to recombine radiatively (owing to the random spatial distribution of the tail states, see below). This is why the Fermi–Dirac function is not applicable to calculate the occupation of luminescence-active states. The crucial problem of the disorder broadening model is thus to determine the distribution function of carriers recombining radiatively in the tail states.

To this end, Boulitrop and Dunstan [13] suppose that a very fast thermalization of non-equilibrium carriers down to the lowest states within a critical volume (surroundings) $V_c$ takes place before the recombination occurs. This volume is driven by the rate of hopping carrier diffusion, i.e. the rate of the non-radiative tunnelling transitions to lower unoccupied states. Let this neighbourhood contain $N$ states (Fig. 9.8) and let us select one reference couple of *e–h* states. The probability $p_n$ of another couple, next to the reference couple, having a lower energy ($E_0$–$E$) decreases exponentially with increasing

[3] Of course, now the wavevector concept and thus the notion of direct and indirect transitions are useless and, moreover, the recombining carriers are *localized*. Nevertheless, the *e–h* recombination is indirect in real space, because the electron and the hole cannot get localized on the same place; see Fig. 9.1(b) or Fig. 9.4.

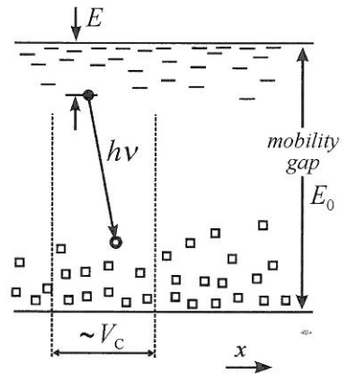


**Fig. 9.8**
Illustrating the calculation of the luminescence occupation probability of the tail states. In a volume $V_c$ around an *e–h* pair with the lowest energy (i.e. with the maximum value of $E$) there are $N$ other couples of states.

$E$, i.e.

$$p_n = e^{-E/E_{c0(v0)}}.$$

This means that the probability of the occurrence of a neighbouring couple with a higher energy $(E_0–E)$ is

$$p_m = (1 - p_n) = (1 - e^{-E/E_{c0(v0)}}).$$

Should the number of such neighbours be $N$, then the occupancy probability of the relevant states will be

$$p_{ec(v)}(E) = (1 - e^{-E/E_{c0(v0)}})^N. \tag{9.12}$$

The density of occupied electron states $R_c(E)$, as a product of the total density of states $g_c(E)$ with the relevant occupation function $p_{ec}$, then reads

$$R_c(E) = g_c(E)p_{ec}(E) \approx e^{-E/E_{c0}}(1 - e^{-E/E_{c0}})^N. \tag{9.13a}$$

Similarly, for the states occupied by holes we get

$$R_v(E_0 - h\nu - E) \approx e^{-(E_0-h\nu-E)/E_{v0}}[1 - e^{-(E_0-h\nu-E)/E_{v0}}]^N \tag{9.13b}$$

and the shape of the emission spectrum is described, in analogy with (5.10), by the convolution

$$I^a_{sp}(h\nu) \approx \int_0^{E_0-h\nu} R_c(E)R_v(E_0 - h\nu - E)\mathrm{d}E. \tag{9.14}$$

Let us note that expression (9.14) does not involve a distribution of radiative lifetimes; it holds for a single value of $\tau_r$.

The material parameters of a-Si:H yield the value of the important parameter $N$ to be $N \approx 50$ (see Problem 1/4). An arbitrary electron thus must not be combined with an arbitrary hole, unlike the recombination of free $e$–$h$ pairs in an indirect bandgap crystalline semiconductor. The values of the occupied tail state densities, calculated with the aid of (9.13),[4] are shown in Fig. 9.9(a). The theoretical lineshape $I^a_{sp}(h\nu)$, obtained with the use of (9.14), is compared with two experimental spectra in Fig. 9.9(b). Obviously the calculated spectrum (curve c) follows well the experimental asymmetry (curves a, b) but is considerably narrower compared to the measured spectra. Taking into account the experimentally determined distribution of radiative lifetimes makes the calculation of $I^a_{sp}(h\nu)$ rather elaborate [14] and the result is represented by curve (d) in Fig. 9.9(b). This curve is wider than the theoretical spectrum (c), but still narrower than the experimental curves. Therefore, the 'disorder broadening' model does not do full justice to the microscopic nature of the luminescence band in disordered semiconductors, and clearly is to be combined with Street's phonon broadening model. A detailed analysis of the applicability of both models in the case of a-Si:H and related alloys can be found in [15].

Another way to improve the disorder broadening model consists in the following reasoning: The involved assumption about full thermalization of

[4] The approximation $[1 - \exp(-x)]^N \cong \exp[-N\exp(-x)]$ has been used.



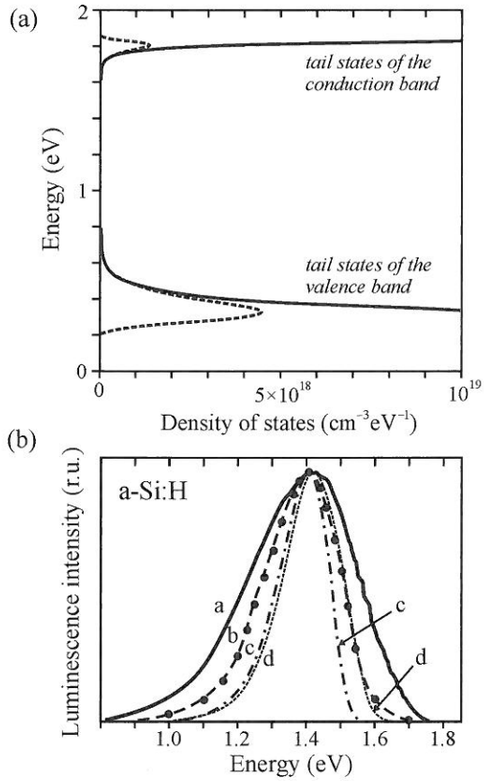


**Fig. 9.9**
(a) The densities of occupied tail states of the conduction and valence bands in a-Si:H (dashed lines) that participate in the radiative recombination. (b) Comparison of two experimental photoluminescence spectra of a-Si:H (curves a, b, $T = 8$ K) with the theoretical shape by Dunstan and Boulitrop, calculated both employing (9.14) for a single value of $\tau_r$(= 10 ms, curve c) and taking into account the experimental distribution function of $\tau_r$ with non-zero width (curve d). After Dunstan and Boulitrop [14].

carriers before recombining in fact discriminates the potential radiative recombination of 'hot carriers', represented by the left transition in Fig. 9.4 (and, to explain the broad distribution curve of lifetimes, the model offers merely a distribution of distances between the localized electrons and holes, like, after all, most other authors). If we admit the existence of the hot luminescence, then the theoretical curves in Fig. 9.9(b) will obviously broaden. The relevant mathematical description, however, would be rather complicated.

## 9.5 Some other properties of luminescence of disordered semiconductors

### 9.5.1 Correlation effects

Excitonic effects play an important role in the luminescence of crystalline solids. The Wannier exciton, a large-radius correlated electron–hole pair moving freely through the lattice, does not exist in disordered materials. However, one may think of an electron–hole correlation of another type. As the wavevector $\mathbf{k}$ of a non-equilibrium carrier is not a good quantum number, its uncertainty can be considered to be infinitely large, $\Delta\mathbf{k} \to \infty$, and the uncertainty relations then for the spatial coordinate $\mathbf{x}$ predict $\Delta\mathbf{x} \to 0$. One can

thus, unlike the crystalline semiconductors, attribute to an electron and a hole a certain space coordinate. We have already met this concept in Figs 9.1 and 9.4 and when discussing the Boulitrop and Dunstan model. Many authors in this context consistently distinguish between recombination of the so-called *geminate* and *non-geminate* $e$–$h$ pairs. Under the geminate pair one understands an electron–hole couple created through the absorption of a given photon in a given site (which means the recombining electron and hole are correlated to a certain extent). The non-geminate pair is represented by an electron and a hole that have originated in different parts of the sample as a consequence of two separated photon absorption events.

Because the photocarrier diffusion length in disordered semiconductors is short, obviously the recombination of geminate pairs dominates at low optical excitation levels when the created $e$–$h$ pairs are sufficiently separated from each other, while at high excitation levels the $e$–$h$ pairs may 'mix up' and the non-geminate recombination may no longer be negligible. One of the central issues of the luminescence of amorphous semiconductors has been for a long time the question of whether radiative recombination (i.e. the tunnelling in the tail states) takes place in arbitrary pairs or in geminate pairs only. Without going into details (we refer to the monograph by Street [1]), at present it is believed that it is the geminate pairs that dominate in luminescence while the annihilation of the non-geminate pairs represents a channel of non-radiative recombination and can be detected for instance via light-induced electron spin resonance.

It is worth noting, however, that Dunstan and Boulitrop in their model [14] do not explicitly differentiate between geminate and non-geminate recombination (even if it can be deduced that implicitly they had in mind the recombination of geminate pairs only). Besides, in the injection electroluminescence, as a matter of fact all $e$–$h$ pairs ought to be considered non-geminate and, consequently, the electroluminescence of amorphous semiconductors would not occur at all. At the same time the very occurrence of electroluminescence in a-Si:H p-i-n structures has been established beyond any doubt for a long time [16] and, even if its intensity is comparatively low, it is applied for instance to studying the microscopic mechanisms of photocarrier recombination and their relations to charge transport processes [17]. Moreover, the electroluminescence of LED structures based on the p-i-n junction in amorphous hydrogenated silicon carbide a-SiC:H exhibits at room temperature a relatively high quantum efficiency ($\sim 10^{-3}\%$) and high brightness (of the order of $10\,\mathrm{cd/m^2}$). The emission is situated in the visible region and these devices have been considered potential candidates for optoelectronic light sources [18]. All these facts are hard to explain if we accept unreservedly the non-radiative recombination of non-geminate pairs.

### 9.5.2 Non-radiative recombination

Multiple passages in this chapter have mentioned possible paths of the non-radiative recombination of $e$–$h$ pairs in amorphous semiconductors. These have been:



1. A recombination mediated by the dangling bonds, i.e. the Shockley–Read recombination at defect levels located approximately in the middle of the bandgap;
2. thermal quenching;
3. recombination of non-geminate $e$–$h$ pairs.

Two additional mechanisms (occurring also in crystalline solids) should be attached, namely:

4. Auger recombination;
5. surface recombination.

Auger recombination gains importance at high excitation intensities (Subsection 6.1.2). Figure 9.10 [19] shows how the relative photoluminescence quantum efficiency $\eta_L$ in a-Si:H and the relevant decay time ($\tau_L$) distribution depend on the excitation photon flux $\phi$; obviously for $\phi$ above a certain level a marked decrease in the luminescence quantum efficiency (not intensity!) occurs and, simultaneously, the decay time gets shorter. This undoubtedly indicates the opening of a new channel of non-radiative recombination, which may be plausibly identified with the Auger process (Problem 9/5): under comparatively high excitation, not only the deep tail states but also shallow localized states close to the mobility edge will be occupied. The latter are characterized by a high spatial density and are thus located close to each other. Under these circumstances the energy of such a recombining $e$–$h$ pair may be transferred either to an electron or to a hole residing in the close neighbourhood. The rate of such an Auger process may even be increased in

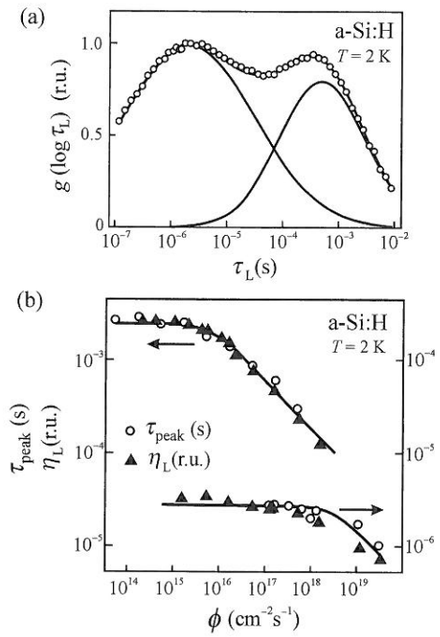


**Fig. 9.10**
(a) The distribution of photoluminescence decay times $\tau_L$, in a-Si:H features, at a very low temperature (here $T = 2\,\mathrm{K}$), two maxima (see also Fig. 9.6(a)). (b) Plot of the temporal location of these maxima and of the relative luminescence quantum efficiency $\eta_L$ versus the excitation photon flux $\phi$. It can be seen how, under high excitation, $\tau_L$ gets shorter and $\eta_L$ is reduced. After Stachowitz *et al.* [19].

comparison with crystalline counterparts because of the breakdown of the **k**-conservation rule.

There is, however, also an alternative point of view. Stachowitz and co-workers [19] have concluded, by analysing the experimental data in Fig. 9.10 that, instead of the Auger process, it is the non-radiative recombination of non-geminate pairs which is responsible for the observed drop of $\tau_L$ and $\eta_L$. They proceed even further, rejecting even the concept of geminate pair radiative recombination and proposing the only possible luminescence centre in a-Si:H to be $e$–$h$ pairs with extremely small separation $R$ between the electron and the hole ($R \sim 0.5$–$1$ nm), therefore a kind of 'small-radius localized exciton'. The occurrence of two maxima in the luminescence decay time distribution (Fig. 9.10(a)) they propose to interpret via recombination of singlet and triplet 'excitons' (whose existence is based on the exchange interaction between spins of closely spaced carriers in the 'exciton'). However, neither can this opinion be easily reconciled with the existence of electroluminescence mentioned in Subsection 9.5.1.

Surface recombination in a thin subsurface layer, owing to the presence of specific unsaturated bonds near the surface, was treated in Subsection 6.1.1. Microscopic features of this non-radiative recombination remain unchanged in disordered materials but, because the thickness of the luminescence 'dead' layer close to the surface depends on the photocarrier diffusion coefficient $D$ which is small in disordered semiconductors, the thickness of this non-luminescent layer $L = \sqrt{D\tau}$ is also very small, typically $L \sim 0.01\,\mu$m at low temperatures. Thus, although the concentration of the subsurface defects is large, the impact of the surface non-radiative recombination on the total luminescence intensity reduction is small ($\sim 10\%$).

Examining once more all of the five mechanisms of non-radiative recombination put forward above, we notice that from the microscopic point of view items (1), (2), (3) and perhaps even (5) can be reduced to a shared basis, which is the occurrence of dangling bonds: In thermal quenching, in surface recombination and perhaps even in non-geminate pair non-radiative recombination, the final dissipation stage of the electronic excitation energy proceeds via a deep defect level. Both kinds of photocarriers meet there in the end, upon accomplishing the diffusion motion, provided they did not find a way to recombine radiatively. A full consensus does not exist in this respect (an alternative chance for the non-geminate pairs is to recombine through direct non-radiative tunnelling between localized states), in any case, however, the role of the dangling non-saturated bonds in non-radiative recombination is substantial.

### 9.5.3 Luminescence of impurities and defects

Till now we have occupied ourselves with the luminescence of pure disordered semiconductors. It is legitimate to ask whether doping of amorphous semiconductors with donors and acceptors can induce novel luminescence processes, similarly to the crystalline analogues (e.g. e–$A^0$, h–$D^0$, etc.). Even though the donor and acceptor energy levels in amorphous materials are broadened due to



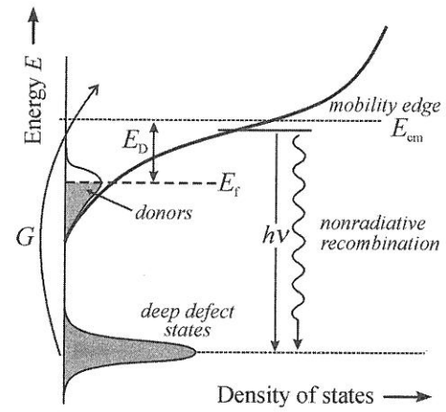


**Fig. 9.11**
Sketch of the density of the donor states (beneath the conduction band bottom, $E_D$ stands for the donor binding energy) and of the deep defect states located approximately in the middle of the bandgap. One conceivable transition representing the defect-related luminescence ($h\nu \sim 0.8$–$0.9$ eV in a-Si:H) is shown. $E_f$ denotes the Fermi level; $G$ indicates the photogeneration rate of non-equilibrium electrons. The shadowed states are occupied in a non-excited semiconductor.

disorder (there is a distribution of the binding energies $E_D$, $E_A$), as indicated in Fig. 9.11, one can certainly imagine for instance a recombination of the type h–$D^0$, when an electron from some of the donor levels recombines radiatively with a hole residing in the valence band tail states.

It has been established experimentally that, e.g., a-Si:H doped with phosphorus or boron actually exhibits a new emission band in the near-infrared region (at $\sim 0.8$–$0.9$ eV against the 'intrinsic' emission peaked at $\sim 1.4$ eV), whose intensity is linked with the presence of the dopants, but the band is due to luminescence of deep defect levels rather than due to transitions e–$A^0$ or h–$D^0$. The introduction of dopants produces new dangling bonds and, accordingly, corresponding deep defect levels roughly in the middle of the band appear. These levels, as we have already stressed several times, mediate predominant non-radiative recombination, but if their concentration is sufficiently increased due to doping, they can manifest themselves through a weak but measurable luminescence (Fig. 9.11). This luminescence therefore originates owing to the radiative recombination of a photocarrier that is localized in the tail states with an oppositely charged photocarrier trapped at the defect level.[5] It should be stressed, of course, that the overall intensity of this long-wavelength emission amounts to a few percent of the principal luminescence band intensity only; the defect levels predominantly quench the 'intrinsic' luminescence and only then substitute it partially by a new channel of radiative recombination.

Figure 9.12(a) displays emission photoluminescence spectra of a-Si:H doped with phosphorus [20]. Obviously, the defect luminescence at $\sim 0.85$ eV can be excited, in line with Fig. 9.11, even by absorption of photons whose energy is considerably less compared to the bandgap width ($E_g \approx 1.5$ eV)). Since the band at $\sim 0.85$ eV is fairly large, the relevant transition has been suggested to be characterized by a strong electron–phonon interaction. This is qualitatively illustrated by the configurational coordinate model sketched

[5] The doping has to be relatively high ($> 10^{17}$ cm$^{-3}$). The Fermi level thereby shifts from the middle of the bandgap close to the relevant mobility edge, and charged dangling bonds along with their correlation energies enter the play. Details go beyond the scope of this book, see Street, R. A. (1991). *Hydrogenated Amorphous Silicon.* Cambridge University Press, Cambridge.

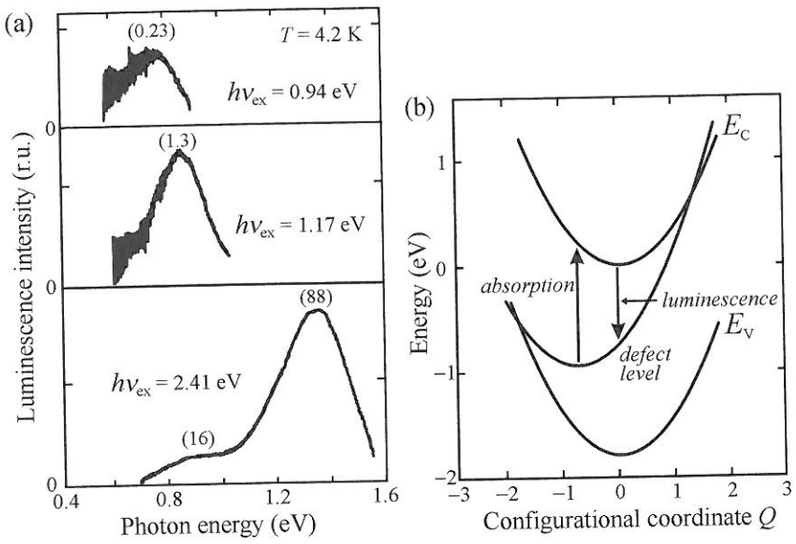


**Fig. 9.12**
(a) Low-temperature emission spectra of a-Si:H doped with phosphorus ($\sim 10^{18}$ cm$^{-3}$), under various excitation photons $h\nu_{ex}$. Numbers in parentheses denote relative intensities of the maxima. (b) Configurational coordinate diagram for the defect luminescence in a-Si:H:P. After Tajima *et al.* [20].

in Fig. 9.12(b). A note may be in order pointing to the resemblance with Fig. 6.1(c), which elucidates an analogous process in a localized centre of a crystalline phosphor.

However, the question of why radiative processes like (e–$A^0$) or (h–$D^0$) have not been observed in amorphous semiconductors is still to be answered here. The reason lies again in the unique feature of these materials—the occurrence of the tail states. From the luminescence point of view, the donor and acceptor states in an excited sample become in fact indistinguishable from the overlapping tail states, 'fusing' with them (see Fig. 9.1(a) or 9.11). This implies that the potential manifestation of their radiative recombination—if any—is included in the main emission band at $\sim 1.4$ eV. Provided the concentration of donors or acceptors is very high ($\sim 10^{19}$–$10^{20}$ cm$^{-3}$), comparable to or even higher than the total density of the tail states, one could perhaps expect some structure superimposed on this emission band. In this case, however, complete quenching of the $\sim 1.4$ eV luminescence due to the high concentration of the defects mostly prevails.

### 9.5.4 Luminescence 'fatigue'

Photoluminescence in amorphous semiconductors may be accompanied by an undesirable adverse effect: gradual fading away of the main emission band, which is observable mainly under relatively high excitation. This is, as generally accepted, due to the Staebler–Wronski effect or the light-induced formation of the dangling bonds; these bonds represent, as already stressed,



powerful quenching centres. An example is displayed in Fig. 9.13, which shows luminescence decay curves of a-Si:H, measured before and after illuminating the sample with an intense cw argon-ion laser (514 nm; 0.54 W; 45 min) [21].[6] A decrease of the luminescence intensity upon illuminating down to about 60 % of the initial value is evident, along with decay shortening. This corresponds to an increased rate of non-radiative transitions. It is worth mentioning that similar experiments performed in nominally pure a-Si:H revealed a moderate increase in intensity of the weak defect luminescence at $\sim 0.85$ eV [22], which fits well the concept of the Staebler–Wronski effect as a phenomenon caused by enhancement of the dangling bond density. Annealing of the sample at a temperature of 150–200°C for one hour usually leads to a complete recovery of the initial photoluminescence intensity.

It is well known that the application potential of amorphous semiconductors has overtaken—already a long time ago—our detailed microscopic understanding of their physical and chemical properties. The present knowledge of the luminescence processes confirms this state of the art—we have been emphasizing throughout this chapter that, as yet, no consensus has been achieved about many issues of both radiative and non-radiative recombination.

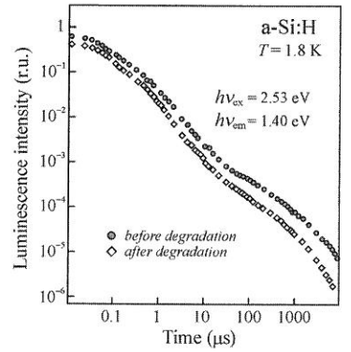


**Fig. 9.13**
Photoluminescence decay curves in a-Si:H (the emission band at $\sim 1.4$ eV, energy of excitation photons $h\nu_{ex} = 2.53$ eV, pulsed excitation 10 ns). Circles and diamonds denote measurements before and after light-induced degradation, respectively. After Hirabayashi *et al.* [21].

## 9.6 Problems

***9/1***: In expression (9.6) for $\eta$ it has been tacitly supposed that all the tail states are occupied, otherwise in the integrals figuring in (9.6) an occupation function $f$ would have appeared (here we apply $f = 1$). Prove that in case this supposition is not valid, one obtains the resulting temperature dependence formally identical with eqn (9.7), only instead of $T$ a temperature $T' > T$ will appear. Determination of the slope $1/T_0$ therefore is not affected.

***9/2***: Assess the tail state width $E_{v0}$ in hydrogen-rich a-Si:H, on the basis of the temperature dependence shown in Fig. 9.2(b). Values of the parameters $p_0$, $\tau_r$ can be found throughout the text of Chapter 9.

***9/3***: Show that (a) if the distribution of luminescence decay times $g(\log \tau_L)$ is very narrow, then expression (9.10) transforms into (9.9), while (b) if $g(\log \tau_L)$ is very broad, it can be approximated as

$$g(\log \tau_L) = g(\log t) \approx i_L(t)t,$$

or simply via multiplying the luminescence intensity $i_L(t)$ by the relevant time decay $t$ related to the end of the excitation event. (For example the curve $g(\log \tau_L)$ in Fig. 9.5 has been determined in this way.) Start from eqn (9.10).

***9/4***: By making use of [13] explain how to estimate the value of the parameter $N$ appearing in eqns (9.12)–(9.14), which represents the number of high-energy ($E_0$–$E$) tail states in the neighbourhood of a particular lower-energy site with a trapped thermalized photocarrier.

[6] The photoluminiscence decay by itself was measured under excitation with a low-peak-power pulsed laser (0.8 kW) in order to avoid distortion of the results owing to the fatigue effect.

*9/5*: With the aid of the equation $dn/dt = G - n/\tau_r - \beta n^2$ comprising Auger non-radiative recombination prove that, at a very high photogeneration rate $G$, drops both in the luminescence decay time and quantum yield occur, driven by a proportion $\sim G^{-1/2}$. Comment: A specific 'extrinsic' Auger recombination of bimolecular type (see eqn (6.8)) in disordered semiconductors is considered.

## References


1. Street, R. A. (1991). *Hydrogenated Amorphous Silicon*. Cambridge University Press, Cambridge.
2. Staebler, D. and Wronski, C. (1977). *Appl. Phys. Lett.*, **31**, 292.
3. Kudrna, J., Malý, P., Trojánek, F., Štěpánek, J., Lechner, T., Pelant, I., Meier, J., and Kroll, U. (2000). *Mater. Sci. Eng. B*, **69–70**, 238.
4. Collins, R. W., Paesler, M. A., and Paul, W. (1980). *Solid State Comm.*, **34**, 833.
5. Luterová, K., Pelant, I., Fojtík, P., Nikl, M., Gregora, I., Kočka, J., Dian, J., Valenta, J., Malý, P., Štěpánek, J., Poruba, A., and Horváth, P. (2000). *Phil. Mag. B*, **80**, 1811.
6. Tsang, C. and Street, R. A. (1979). *Phys. Rev. B*, **19**, 3027.
7. Wang, W. and Fritzsche, H. (1989). *Photoluminescence in a-Si:H films and multilayers*. In *Advances in Semiconductors*, Vol. 1, *Amorphous Silicon and Related Materials*, Vol. B (ed H. Fritzsche), p. 779. World Scientific, Singapore.
8. Oheda, H. (1993). *J. Non-Crystal. Solids*, **164–166**, 559.
9. Koós, M., Pócsik, I., and Tóth, L. (1993). *J. Non-Crystal. Solids*, **164–166**, 1151.
10. Street, R. A. and Biegelsen, D. K. (1980). *Solid State Comm.*, **33**, 1159.
11. Deki, H., Miyazaki, S., Ohmura, M., and Hirose, M. (1993). *J. Non-Crystal. Solids*, **164–166**, 841.
12. Street, R. A. (1978). *Phil. Mag. B*, **37**, 35.
13. Boulitrop, F. and Dunstan, D. J. (1983). *Phys. Rev. B*, **28**, 5923.
14. Dunstan, D. J. and Boulitrop, F. (1984). *Phys. Rev. B*, **30**, 5945.
15. Searle, T. M. and Jackson, W. A. (1989). *Phil. Mag. B*, **60**, 237.
16. Pankove, J. E. and Carson, D. E. (1976). *Appl. Phys. Lett.*, **29**, 620.
17. Wang, K., Han, D., Kemp, M., and Silver, M. (1993). *Appl. Phys. Lett.*, **62**, 157.
18. Kruangam, D. (1991). *Amorphous and microcrystalline silicon–carbide alloy light–emitting diodes: physics and properties.* In: *Amorphous & Microcrystalline Semiconductor Devices* (ed J. Kanicki), p. 195. Artech House, Boston.
19. Stachowitz, R., Schubert, M., and Fuhs, W. (1998). *J. Non-Crystal. Solids*, **227–230**, 190.
20. Tajima, M., Okushi, H., Yamasaki, S., and Tanaka, K. (1986). *Phys. Rev. B*, **33**, 8522.
21. Hirabayashi, I., Morigaki, K., and Nitta, S. (1980). *Jap. J. Appl. Phys.* **19**, L357.
22. Tajima, M., Okyama, H., Okushi, H., Yamasaki, S., and Tanaka, K. (1989). *Jap. J. Appl. Phys.*, **28**, L1086.


# Stimulated emission

# 10



Stimulated emission can be viewed as a special case of luminescence. Its character conforms to the definition of luminescence (the excess electromagnetic radiation when compared to the equilibrium radiation as described by Planck's law, featuring simultaneously a 'sufficiently long' lifetime), although the thermodynamic conditions necessary for its occurrence differ fundamentally from the common occupancy of electronic states in spontaneous luminescence processes. A population inversion of energy levels, a state diametrically opposed to thermodynamic equilibrium, needs to be achieved. That is why, among other things, the spectral distribution of stimulated emission cannot be described using relations (5.9), (7.11) or (7.16), as these relations are valid provided that only minute variations from the equilibrium occupancy of states occur. It is thus obvious that the description of stimulated emission needs to be based on a completely different principle. Apart from the thermodynamic non-equilibrium, the nonlinear character of this optical process starts to be of particular importance.

In this chapter, we will first formulate the conditions necessary for the occurrence of stimulated emission in bulk semiconductors. Then, we will show how stimulated emission can originate in an electron–hole plasma (EHP) and discuss possible contributions of excitons and excitonic complexes to stimulated emission. Finally, the methods employed for the study of optical gain will be described.

## 10.1 Spontaneous versus stimulated emission. Optical gain

The phenomenon of stimulated emission is generally unconsciously perceived as the fundamental principle underlying the operation of all lasers. In luminescence spectroscopy, stimulated emission can be treated from two diametrically opposed points of view. If a particular phosphor is studied as a potential new active laser medium, any manifestation of stimulated emission is warmly welcome. If, on the other hand, importance is put on the basic research of the fundamentals of radiative recombination processes, should (unintentionally) stimulated emission arise, the emission spectrum or luminescence dynamics